VACUUM FACILITY AT LNF-INFN FOR PRESENT AND FUTURE ACCELERATORS

L. Spallino*, D. Alesini, M. Angelucci, S. Bini, P. Chimenti, R. Cimino, G. De Bernardis, S. De Biase, G. Di Raddo, R. Di Raddo, A. Liedl, V. Lollo, M. Pietropaoli, V. Sciarra, G. Viviani, M. Zottola
INFN Laboratori Nazionali di Frascati, Frascati, Italy

Abstract

The management and characterization of materials intended for vacuum applications play a key role in ensuring the reliability and performance of modern particle accelerator systems. The LNF-INFN vacuum laboratory, originally established to support the development of components for several accelerator projects, has progressively evolved into a reference infrastructure serving current and future flagship projects, including EuPRAXIA and ET. The facility hosts equipment dedicated to the preparation, cleaning, and thermal treatment of ultra-high-vacuum components, as well as systems for material outgassing characterization. In collaboration with MaSSLab at DAΦNE-L, the laboratory also offers advanced surface analysis techniques. This work presents the main capabilities of the facility and illustrates their application across different project contexts.

INTRODUCTION

Vacuum systems are essential components of modern particle accelerators, as beam lifetime, emittance preservation, and overall machine stability depend critically on both static and dynamic vacuum performance [1, 2]. Achieving the ultra-high-vacuum (UHV) conditions required by present and next-generation facilities necessitates stringent control over gas loads, surface properties, material history, and environmental exposure through fabrication and installation. At INFN-LNF, the long-standing support to accelerator development - from the Electron Synchrotron and Adone to DAΦNE and SPARC - has led to the establishment of a specialized vacuum infrastructure. Built upon many years of accumulated experience, this infrastructure has now reached a level of maturity that enables its effective contribution to major national and international initiatives, including EuPRAXIA@SPARC_LAB [3] and the Einstein Telescope (ET) [4]. In this context, the present technical note aims to document the facility and its capabilities, with particular emphasis on its adherence to widely adopted standards in the UHV field [1, 5, 6]. Ensuring consistency with established procedures, datasets, and operational practices is essential for meaningful comparison and exchange with other laboratories, thus supporting collaborative development and benchmarking within the broader UHV community, including large-scale infrastructures for both accelerator and gravitational-wave research [1, 7–9]. The motivation for this technical note arises from the increasing need to understand the material-dependent mechanisms governing vacuum behavior, including desorption of surface-adsorbed species, diffusion-limited outgassing, and beam-induced processes such as photon-, ion-, and electron-stimulated desorption. These phenomena are strongly affected by material composition, surface finishing, cleanliness, thermal treatments, and storage conditions, all of which influence gas-release kinetics and surface reactivity [10–14]. As emerging facilities impose ever more stringent vacuum specifications, laboratories capable of controlled preparation, characterization, and qualification of UHV components under realistic conditions become indispensable. A systematic understanding of material-driven vacuum processes is now crucial not only for accelerator reliability but also for the broader community of advanced UHV-based scientific infrastructures. This is particularly relevant for large-scale projects such as ET, whose long-baseline interferometers rely on ultraclean, ultra-stable vacuum environments [4, 15, 16]. The INFN-LNF facility includes a UHV preparation and cleaning area equipped with large-volume ultrasonic tanks, a vacuum-brazing furnace, a heat-treatment furnace, and an outgassing-rate characterization system. In collaboration with the Material Surface Science Laboratory (MaSSLab) at DAΦNE-L, additional surface-analysis tools for both room-temperature (RT) and cryogenic operation (LT) are also available. An overview of the facility's equipment, measurement capabilities, and representative project applications is provided below.

VACUUM FACILITY

Cleaning Room

The laboratory features a dedicated cleaning room equipped with two ultrasonic tanks with temperature control ($50 \times 50 \times 50$ cm^3 and $200 \times 50 \times 40$ cm^3) and a large oven for filtered air drying (T_{max}~200°C). Some pictures are reported in Fig. 1.

These systems enable the cleaning of vacuum chambers and components (up to medium/large sizes, compatible with the tank dimensions) using reproducible procedures developed for UHV applications and consistent with established methods reported in the literature [1, 10, 13, 14]. UHV compatibility is assessed by outgassing measurements and Residual Gas Analysis (RGA), as described below. As a representative example, the procedure developed for cleaning stainless steel to meet UHV requirements is presented.

- *Pre-cleaning removal of gross contamination*. Remove any gross contamination. Wash and swab the surface using an alkaline detergent (Almeco 19, ~2% dilution) in hot water (T~60°C). Rinse with RT water without

* luisa.spallino@lnf.infn.it

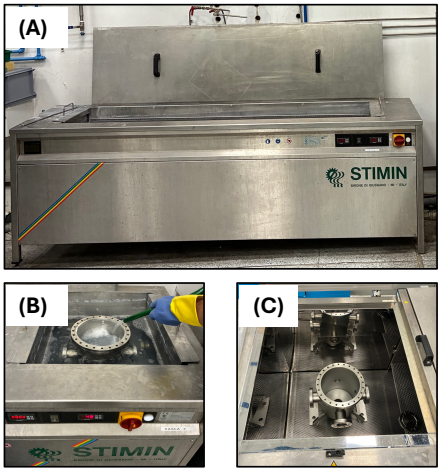

Figure 1: (A) and (B): ultrasonic tanks in the cleaning room; (C) oven for vacuum component drying.

detergent, ensuring that all visible contamination and solvent residues are completely removed.

- *Ultrasonic bath*. Immerse the component in a bath of hot water (T∼50°C) and alkaline detergent (Almeco 19, ∼1% dilution) with ultrasonic agitation for 15 minutes. For complex geometries, repeat the ultrasonic bath two or three times. After ultrasonic cleaning, gradually add room temperature (RT) water to the bath to allow slow cooling.

- *Rinsing*. Rinse first with tap water at RT until all traces of detergent are removed. Follow with a final rinse using demineralised water.

- *Drying*. Dry the component by blowing with N_2 and then placing it in an oven with filtered air at T∼60°C. Drying time depends on the shape and geometry of the component and may range from one hour to 12 hours.

Furnaces

Two furnaces are available in the laboratory to perform thermal treatments in HV of medium/large components (Fig. 2). One, (A), is equipped with a thermal chamber of 400 mm diameter and 1500 mm length, and can operate up to 450°C. The other one, (B), has a thermal chamber of 400 mm diameter and 1300 mm height, with a maximum continuous operating limit at 1200°C. This furnace also allows controlled-atmosphere heat treatments (Ar, N_2) at a pressure ranging from 1 to 10 mbar. The ultimate vacuum for both is below $1{\cdot}10^{-6}$ mbar, while during operation the vacuum level can reach maximum $1{\cdot}10^{-5}$ mbar. For both, the thermal ramp can be adjusted at will, depending on the treatment.

Such furnaces are routinely employed to process components to be installed in all LNF-INFN UHV facilities, ensuring the removal of surface contaminants, enabling stainless-steel and copper firing, and performing high-quality brazing of custom-made parts. Within the R&D activities of the EuPRAXIA@SPARC_LAB and related

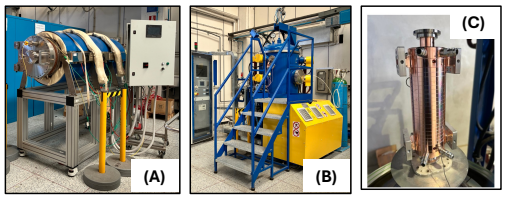

Figure 2: Pictures of the two HV furnaces hosted in the laboratory for thermal treatments at T_{max}∼450°C (A) and T_{max}∼1200°C (B). (C): 20-cell RF prototype of the X-band accelerating structure after brazing [17].

projects [17], these furnaces represent a key asset for both prototyping and potentially producing X-band accelerating structures such as the one shown in Fig. 2(C) [17–22].

Outgassing Rate System

A dedicated apparatus based on the throughput method is available for measuring the total outgassing rates of materials and assemblies, using a calibrated conductance system and a Residual Gas Analyzer (RGA). As illustrated in the schematic in the upper part of Fig. 3, the setup features a measurement chamber (base pressure∼$2{\cdot}10^{-11}$ mbar) connected to two distinct sample chambers. These chambers differ in geometric volume - and therefore internal surface area - making one more suitable for high-outgassing materials (the smaller chamber, C_1) and the other for low-outgassing materials (the larger chamber, C_2). Each sample chamber is linked to the measurement chamber by a separating valve; a calibrated conductance orifice (C=10 $l{\cdot}s^{-1}$, N_2 equivalent) is installed at each valve. The system includes various

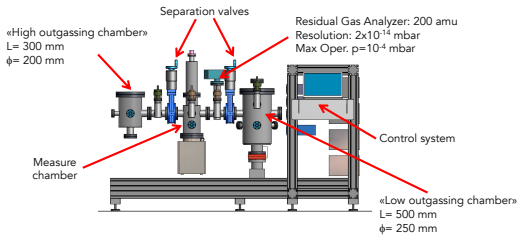

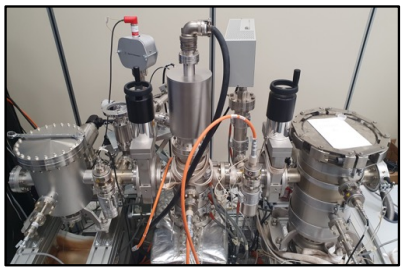

Figure 3: Top: schematic representation of the experimental apparatus dedicated to outgassing rate measurements. Bottom: pictures of the system in the laboratory.

pressure gauges, namely Pirani gauges for rough vacuum and cold cathodes for outgassing measurements (with an uncertainty of approximately 30%). The background specific outgassing rates are q_{C_1}∼10^{-12} mbar·l·s^{-1}·cm^{-2} for C_1 and q_{C_2}∼10^{-14} mbar·l·s^{-1}·cm^{-2} for C_2. The measurement chamber is equipped with a mass spectrometer for

RGA analysis (up to 200 amu), enabling the assessment of outgassing in terms of the partial pressures of released contaminants. Additionally, the apparatus includes heaters and temperature controllers to perform temperature-dependent outgassing measurements. The data produced by this apparatus provide a quantitative basis for material screening and component qualification in UHV environments. Within this framework, access to a a state-of-the-art apparatus for quantitative outgassing-rate measurements is essential since it enables the assessment of the vacuum compliance of materials and assemblies developed for the future EuPRAXIA-SPARC_LAB infrastructure. An example is the study on the vacuum behaviour of the accelerating structures (as the one reported in Fig. 2(C)), whose partial-pressure fingerprints can be directly extracted via RGA (data not reported). Furthermore, the same experimental infrastructure supports the validation of materials and components foreseen for deployment in the future ET cryogenic towers, where stringent constraints on molecular-flux budgets and residual-gas composition require precise quantification of contaminant species under controlled thermal and vacuum conditions.

MATERIAL SURFACE SCIENCE LABORATORY

Close collaboration with MaSSLab at DAΦNE-L significantly enhances capabilities to investigate surface physics, both at RT and at LT. At the core of the laboratory's infrastructure is a system comprising a μ-metal main analysis chamber operating at a base pressure of $\sim 2\times10^{-10}$ mbar. This chamber is connected to a preparation chamber via a gate valve and features a fast-entry lock with an internal transfer mechanism that enables sample introduction without breaking vacuum. A picture of the system is reported in Fig. 4. The analysis chamber is equipped with a helium-cooled cryogenic manipulator capable of stabilizing sample temperatures between 10 and 400 K. Gas dosing can be performed through a leak valve and a custom-made dosing tube. The system supports temperature-programmed desorption (TPD) measurements via a quadrupole mass spectrometer (up to 100 amu). Low-energy electron guns (5–2000 eV) allow controlled electron irradiation of surfaces for both Secondary Electron Yield (SEY) measurements - conducted using high-precision picoammeters - and Electron Stimulated Desorption (ESD) experiments. A key feature of this system is its capability for in-situ X-ray Photoelectron Spectroscopy (XPS), enabled by dedicated X-ray sources and a hemispherical electron analyzer. The preparation chamber includes equpments for sample sputtering and is set up with an evaporator for physical-vapor-deposition, allowing the preparation of substrates under controlled conditions without exposure to ambient atmosphere. More details can be found in literature [23–27].Over the years, MASSLab at DAΦNE-L has supported, and continues to support, a broad range of scientific domains - from the mitigation of electron-cloud effects in accelerator environments (LHC, FCC, EIC) [24,26–33] to the study of electron-induced chemistry in cryosorbed molecular systems relevant to the interstellar medium [34]. The insights gained through these investigations have enabled the proposal of active mitigation strategies for frost formation and electrostatic charging on the cryogenic optics of ET. These strategies are based on controlled low-energy electron irradiation and detailed knowledge of the SEY properties of relevant materials [15, 35, 36].

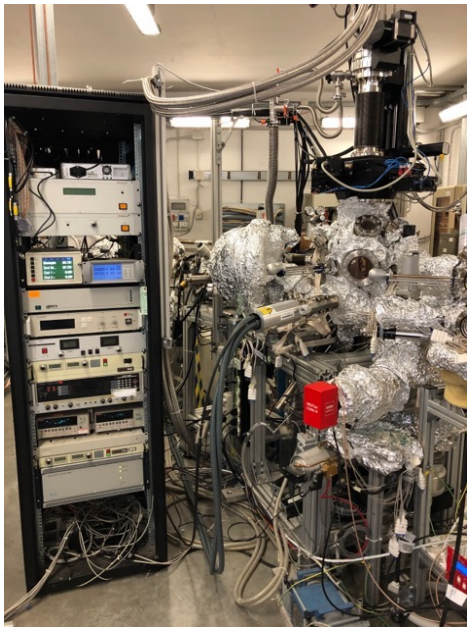

Figure 4: Picture of one of the MaSSLab at DAΦNE-L measuring system.

CONCLUSION

The LNF-INFN vacuum facility represents a comprehensive infrastructure enabling material preparation, thermal treatment, vacuum qualification and surface analysis for accelerator and cryogenic technologies. Its combination of UHV cleaning, furnaces, outgassing setups and advanced surface science instrumentation - strengthened by collaboration with MaSSLab at DAΦNE-L - provides essential support to ongoing and future large scale projects. With the increasing complexity of accelerator components and the stringent requirements of next generation facilities, the laboratory will continue to play a crucial role in developing, testing and validating materials and assemblies under controlled vacuum conditions.

REFERENCES

[1] O. B. Malyshev, *Vacuum in Particle Accelerators: Modelling, Design and Operation of Beam Vacuum Systems*. Weinheim, Germany: Wiley-VCH, 2020. doi:10.1002/9783527809134

[2] V. Baglin and R. Kersevan, "Vacuum systems", in *Proc. Joint Universities Accelerator School (JUAS): Courses and Exercises*, Geneva, Switzerland, 2024, pp. 1259–1338. doi:10.23730/CYRSP-2024-003.1259

[3] D. Alesini *et al.*, "EuPRAXIA@SPARC_LAB Technical Design Report", Open Access Repository, Rep., Feb. 2026. doi:10.15161/oar.it/k57qz-5qk09

[4] ET Science Team, "Einstein gravitational wave Telescope conceptual design study", Zenodo, Rep. ET-0106C-10, Jun. 2011. doi:10.5281/zenodo.3911261

[5] J. M. Lafferty, *Foundations of Vacuum Science and Technology*. New York, NY, USA: Wiley, 1998. 978-0471175933

[6] P. A. Redhead, *Extreme high vacuum*. CERN, Geneva, Switzerland, Rep. OPEN-2000-281, Aug. 1999. doi:10.5170/CERN-1999-005.213

[7] J. Abada *et al.*, "FCC-hh: The Hadron Collider", *Eur. Phys. J. Spec. Top.*, vol. 228, pp. 755–1107, 2019. doi:10.1140/epjst/e2019-900087-0

[8] M. Punturo *et al.*, "The Einstein Telescope: a third-generation gravitational wave observatory", *Class. Quantum Grav.*, vol. 27, no. 19, pp. 194002, 2010. doi:10.1088/0264-9381/27/19/194002

[9] The LIGO Scientific Collaboration *et al.*, "Advanced LIGO", *Class. Quantum Grav.*, vol. 32, no. 7, pp. 074001, 2015. doi:10.1088/0264-9381/32/7/074001

[10] K. J. Middleman, J. D. Herbert, and R. J. Reid, "Cleaning stainless steel for use in accelerators–Phase 1", *Vacuum*, vol. 81, no. 6, pp. 793–798, 2007. doi:10.1016/j.vacuum.2005.11.057

[11] R. Grinham and A. Chew, "A review of outgassing and methods for its reduction", *Appl. Sci. Converg. Technol.*, vol. 26, no. 5, pp. 95–109, 2017. doi:10.5757/ASCT.2017.26.5.95

[12] P. Chiggiato, "Outgassing properties of vacuum materials for particle accelerators", arXiv:2006.07124, 2020. doi:10.48550/arXiv.2006.07124

[13] M. Taborelli, "Cleaning and surface properties", arXiv:2006.01585, 2020. doi:10.48550/arXiv.2006.01585

[14] M. Taborelli, "Surface finishing and coatings for accelerator vacuum applications", arXiv:2506.23691, 2025. doi:10.48550/arXiv.2506.23691

[15] L. Spallino *et al.*, "Cryogenic vacuum considerations for future gravitational wave detectors", *Phys. Rev. D*, vol. 104, p. 062001, 2021. doi:10.1103/PhysRevD.104.062001

[16] A. Grado *et al.*, "Ultra high vacuum beam pipe of the Einstein Telescope project: Challenges and perspectives", *J. Vac. Sci. Technol. B*, vol. 41, p. 024201, 2023. doi:10.1116/6.0002323

[17] F. Cardelli *et al.*, "Preliminary results on X-band structures for the EuPRAXIA@SPARC_LAB project", in *Proc. IPAC'24*, Nashville, TN, USA, May 2024, pp. 1436–1439. doi:10.18429/JACoW-IPAC2024-TUPR10

[18] F. Cardelli *et al.*, "Advancements in X-band technology at the TEX facility at INFN-LNF", in *Proc. IPAC'24*, Nashville, TN, USA, May 2024, pp. 1421–1424. doi:10.18429/JACoW-IPAC2024-TUPR02

[19] D. Alesini *et al.*, "Design, realization and high power RF test of the new brazed free C band photo-gun", in *Proc. IPAC'24*, Nashville, TN, USA, May 2024, pp. 2929–2932. doi:10.18429/JACoW-IPAC2024-THAN1

[20] F. Cardelli *et al.*, "The TEX facility upgrade at INFN-LNF", presented at IPAC'26, Deauville, France, May 2026, paper MOP7008, this conference.

[21] F. Cardelli *et al.*, "Preliminary R&D on X-band components for the X-band based user facility EuPRAXIA@SPARC_LAB", *Eur. Phys. J. Spec. Top.*, vol. 234, p. 8137, 2026. doi:10.1140/epjs/s11734-025-01828-0

[22] D. Alesini *et al.*, "Design, realization, and testing of a brazing-free C-band radio frequency photogun", *Phys. Rev. Accel. Beams*, vol. 29, p. 012001, 2026. doi:10.1103/jrth-j9sf

[23] R. Cimino and T. Demma, "Electron cloud in accelerators", *Int. J. Mod. Phys. A*, vol. 29, no. 17, p. 1430023, 2014. doi:10.1142/S0217751X14300233

[24] R. Cimino *et al.*, "Detailed investigation of the low energy secondary electron yield of technical Cu and its relevance for the LHC", *Phys. Rev. ST Accel. Beams*, vol. 18, p. 051002, 2015. doi:10.1103/PhysRevSTAB.18.051002

[25] L. A. Gonzalez, M. Angelucci, R. Larciprete, and R. Cimino, "The secondary electron yield of noble metal surfaces", *AIP Adv.*, vol. 7, p. 115203, 2017. doi:10.1063/1.5000118

[26] L. Spallino, M. Angelucci, and R. Cimino, "Thermal desorption of cryopumped gases from laser treated copper", *Phys. Rev. Accel. Beams*, vol. 23, p. 063201, 2020. doi:10.1103/PhysRevAccelBeams.23.063201

[27] M. Angelucci, A. Novelli, L. Spallino, A. Liedl, and R. Cimino, "Minimum thickness of carbon coating for multipacting suppression", *Phys. Rev. Research*, vol. 2, p. 032030(R), 2020. doi:10.1103/PhysRevResearch.2.032030

[28] R. Cimino *et al.*, "Can low-energy electrons affect high-energy physics accelerators?", *Phys. Rev. Lett.*, vol. 93, p. 014801, 2004. doi:10.1103/PhysRevLett.93.014801

[29] R. Cimino *et al.*, "Nature of the decrease of the secondary-electron yield by electron bombardment and its energy dependence", *Phys. Rev. Lett.*, vol. 109, p. 064801, 2012. doi:10.1103/PhysRevLett.109.064801

[30] R. Cimino, V. Baglin, and F. Schäfers, "Potential remedies for the high synchrotron-radiation-induced heat load for future highest-energy-proton circular colliders", *Phys. Rev. Lett.*, vol. 115, p. 264804, 2015. doi:10.1103/PhysRevLett.115.264804

[31] L. Spallino, M. Angelucci, R. Larciprete, and R. Cimino, "On the compatibility of porous surfaces with cryogenic vacuum in future high-energy particle accelerators", *Appl. Phys. Lett.*, vol. 114, p. 153103, 2019. doi:10.1063/1.5085754

[32] R. Cimino, M. Angelucci, L. A. Gonzalez, and R. Larciprete, "SEY and low-energy SEY of conductive surfaces", *J. Electron Spectrosc. Relat. Phenom.*, vol. 241, p. 146876, 2020. doi:10.1016/j.elspec.2019.06.008

[33] E. La Francesca *et al.*, "Reflectivity and photoelectron yield from copper in accelerators", *Phys. Rev. Accel. Beams*, vol. 23, p. 083101, 2020. doi:10.1103/PhysRevAccelBeams.23.083101

[34] R. Dupuy *et al.*, “X-ray photodesorption from water ice in protoplanetary disks and X-ray-dominated regions”, *Nat. Astron.*, vol. 2, pp. 796–801, 2018. doi:10.1038/s41550-018-0532-y

[35] L. Spallino *et al.*, “Can electrons neutralize the electrostatic charge on test mass mirrors in gravitational wave detectors?”, *Phys. Rev. D*, vol. 105, p. 042003, 2022. doi:10.1103/PhysRevD.105.042003

[36] L. Spallino, M. Angelucci, A. Liedl, and R. Cimino, “The role of secondary electron yield in mitigating electrostatic charging in future gravitational waves detectors”, *Vacuum*, vol. 233, p. 113969, 2025. doi:10.1016/j.vacuum.2024.113969